Cancer Letters 388 (2017) 34–42

Contents lists available at ScienceDirect

Cancer Letters

journal homepage: www.elsevier.com/locate/canlet

Original Article

# Doxorubicin-induced mitophagy contributes to drug resistance in cancer stem cells from HCT8 human colorectal cancer cells

Chen Yan [a], Lan Luo [a], Chang-Ying Guo [a, b], Shinji Goto [a], Yoshishige Urata [a], Jiang-Hua Shao [c], Tao-Sheng Li [a, *]

[a] Department of Stem Cell Biology, Nagasaki University Graduate School of Biomedical Sciences, 1-12-4 Sakamoto, Nagasaki 852-8523, Japan
[b] Department of Thoracic Surgery, Jiangxi Cancer Hospital, Nanchang 330029, China
[c] Department of General Surgery, The Second Affiliated Hospital of Nanchang University, Nanchang 330006, China

ARTICLE INFO

*Article history:*
Received 30 August 2016
Received in revised form
2 November 2016
Accepted 17 November 2016

*Keywords:*
Cancer stem cells
Drug resistance
Mitophagy
BNIP3L
Autophagy

ABSTRACT

Cancer stem cells (CSCs) are known to be drug resistant. Mitophagy selectively degrades unnecessary or damaged mitochondria by autophagy during cellular stress. To investigate the potential role of mitophagy in drug resistance in CSCs, we purified $CD133^+/CD44^+$ CSCs from HCT8 human colorectal cancer cells and then exposed to doxorubicin (DXR). Compared with parental cells, CSCs were more resistant to DXR treatment. Although DXR treatment enhanced autophagy levels in both cell types, the inhibition of autophagy by ATG7 silencing significantly increased the toxicity of DXR only in parental cells, not in CSCs. Interestingly, the level of mitochondrial superoxide was detected to be significantly lower in CSCs than in parental cells after DXR treatment. Furthermore, the mitophagy level and expression of BNIP3L, a mitophagy regulator, were significantly higher in CSCs than in parental cells after DXR treatment. Silencing BNIP3L significantly halted mitophagy and enhanced the sensitivity to DXR in CSCs. Our data suggested that mitophagy, but not non-selective autophagy, likely contributes to drug resistance in CSCs isolated from HCT8 cells. Further studies in other cancer cell lines will be needed to confirm our findings.

© 2016 Elsevier Ireland Ltd. All rights reserved.

## Introduction

In recent decades, a stem cell-like subpopulation known as "cancer stem cells" (CSCs) has been found in various types of solid tumors [1]. These CSCs have the stem cell properties of self-renewal and differentiation, giving rise to tumor therapeutic resistance, metastasis and recurrence [1]. In colorectal cancer, the limitation of chemotherapy has been ascribed primarily to the drug resistance of CSCs [2,3], but the relevant mechanisms are not completely understood.

Mitochondria are crucial organelles for energy metabolism, regulation of cell signaling and apoptosis [4]. To avoid cell damage and to maintain cellular homeostasis, the cell has evolved complex systems for the quality control of mitochondria. One of these systems, mitophagy, selectively degrades excessive or damaged mitochondria by autophagy in response to various stresses [5,6]. Dysregulation of mitophagy may contribute to cancer progression and cell survival in various types of tumors [6,7]. It has recently been found that the inhibition of mitophagy enhances chemosensitivity in cancer cells [8], but the role of mitophagy in the drug resistance of CSCs remains unclear.

As a DNA-damaging agent, doxorubicin (DXR) is regularly used in anticancer therapy. It has been reported that DXR intercalates into not only nuclear DNA but also mitochondrial DNA [9]. In addition, DXR is believed to cause toxicity by inducing mitochondrial dysfunction and enhancing superoxide formation [10,11]. As the evasion of DXR-induced mitochondrial dysfunction may be a

*Abbreviations:* ATG7, autophagy related 7; BNIP3L, BCL2/adenovirus E1B 19 kDa protein-interacting protein 3-like; CSCs, cancer stem cells; DXR, doxorubicin; DAPK1, death-associated protein kinase 1; DNA, deoxyribonucleic acid; ECL, enhanced chemiluminescence; ERK1/2, extracellular signal-regulated protein kinases 1 and 2; FADD, Fas-associated protein with death domain; FITC, fluorescein isothiocyanate; HRP, horseradish peroxidase; MAP1LC3B/ LC3B, microtubule-associated proteins 1 light chain 3B; MAPKs, mitogen-activated protein kinases; MTT, 3-(4,5-dimethylthiazol-2-yl)-2,5-diphenyltetrazolium bromide; PARP, poly ADP ribose polymerase; PCR, polymerase chain reaction; PINK1, PTEN-induced putative kinase 1; RNA, ribonucleic acid; RPMI 1640, Roswell Park Memorial Institute 1640; TNFSF10, tumor necrosis factor superfamily member 10; TOMM20, translocase of outer mitochondrial membrane 20.

* Corresponding author. Fax: +81 95 819 7100.
*E-mail address:* litaoshe@nagasaki-u.ac.jp (T.-S. Li).

http://dx.doi.org/10.1016/j.canlet.2016.11.018
0304-3835/© 2016 Elsevier Ireland Ltd. All rights reserved.

potential mechanism of drug resistance, we hypothesized that mitophagy contributes to DXR resistance in CSCs through the down-regulation of mitochondria-related cell death.

CD133 and CD44 are among the most useful markers for the identification of colorectal CSCs [1,12]. In this study, we isolated the $CD133^+/CD44^+$ CSCs from parental HCT8 colorectal cancer cells, and then compared their mitophagy activity and DXR sensitivity. Our results showed that mitophagy, but not non-selective autophagy, likely contributes to DXR resistance in CSCs isolated from HCT8 cells.

## Materials and methods

### *Cell culture*

The HCT8 human colorectal cancer cell line was used for experiments. Cells were maintained in RPMI 1640 medium (#189-02025, Wako) with 10% fetal bovine serum (#12483-020, Gibco) and 1% penicillin–streptomycin (#15140122, Gibco) at 37 °C in a humidified atmosphere with 5% $CO_2$ and 95% air.

### *Purification of $CD133^+/CD44^+$ CSCs*

We separated the $CD133^+/CD44^+$ cells by using the Magnetic Cell Sorting system (autoMACS; Miltenyi Biotec) [13]. Briefly, a single-cell suspension of HCT8 cells was incubated with magnetic microbeads-conjugated with an anti-human CD44 antibody (#130-095-194, Miltenyi Biotec) for 30 min. After washing, the $CD44^+$ cells were separated using the Magnetic Cell Sorting system (autoMACS; Miltenyi Biotec). The purified $CD44^+$ cells were expanded and then harvested as a single-cell suspension to be incubated with magnetic microbeads-conjugated with an anti-human CD133 antibody (#130-050-801, Miltenyi Biotec) for 30 min. After washing, the $CD133^+$ cells were separated using the Magnetic Cell Sorting system as described above. This two-step isolation enabled us to obtain a sufficient number of $CD133^+/CD44^+$ CSCs for the experiments.

To verify the purity of the isolated $CD133^+/CD44^+$ CSCs, cells were stained according to the supplied antibody protocols. Mouse anti-human CD133/1 (Clone: AC133)-PE (#130-080-801, Miltenyi Biotec) and mouse anti-human CD44 (Clone: DB105)-FITC (#130-095-195, Miltenyi Biotec) were used, and flow cytometry analysis was performed using a FACSCalibur instrument (Becton Dickinson). Mouse IgG1-PE (#130-092-212, Miltenyi Biotec) and mouse IgG1-FITC (#130-092-213, Miltenyi Biotec) were used as negative control.

### *Cytotoxicity assays*

Cells were seeded in 96-well culture plates at a density of $2 \times 10^4$ cells per well and cultured overnight. The cells were then treated with various concentrations (0, 1, 3, 5 and 10 μM) of DXR (#040-21521, Wako) for 24 h. After DXR treatment, cytotoxicity assays were performed using the Cell Proliferation Kit I (MTT) (#11465007001, Roche Life Science). Briefly, MTT was added and incubated for 4 h. Then, the formation of formazan from MTT was stopped by adding solubilization solution, and the absorbance of formazan was measured at 570 nm using a microplate reader (Multiskan Fc, Thermo Fisher Scientific). We used the optical density (OD) value of cells with vehicle treatment as a normalization control (100%).

### *Apoptosis assays*

FITC-Annexin V and propidium iodide (PI) staining were performed using the Annexin V-FITC Apoptosis Detection Kit (#IM2375, Beckman Coulter) [13]. Briefly, cells were harvested as a single-cell suspension. Then, 5 μL of FITC-Annexin V solution and 2.5 μL dissolved PI were added to 100 μL of the cell suspension. The mixture was then incubated on ice for 10 min in the dark. Then, 400 μL of ice-cold binding buffer was added to the preparations and gently mixed, followed by flow cytometry analysis using a FACSCalibur instrument (Becton Dickinson).

### *Time-course experiments*

Cells were seeded in culture dishes and cultured overnight. The cells were then treated with 10 μM of DXR for 0, 3, 6, 12 and 24 h. After treatment, the cell lysates were collected at the indicated time points.

### *Antibodies and reagents*

The LC3B antibody (#NB100-2220) was obtained from Novus Biologicals. The α-tubulin (#3873), PARP (#9542), cleaved PARP (#5625), caspase-3 (#9665), cleaved caspase-3 (#9664), caspase-7 (#12827), cleaved caspase-7 (#8438), ATG7 (#2631), PINK1 (#6946), parkin (#4211), BNIP3L (#12396), and phospho-ERK1/2 (Thr202/Tyr204) (#4370) antibodies were purchased from Cell Signaling Technology. The β-actin antibody (#A2228) was obtained from Sigma–Aldrich. The TOMM20 antibody (#sc-17764) was obtained from Santa Cruz Biotechnology. Anti-mouse (#P0260) and anti-rabbit (#P0448) HRP-coupled secondary antibodies were obtained from Dako. DAPI (4′, 6-diamidino-2-phenylindole) (#D21490), anti-mouse (#A-11030) Alexa Fluor 546 and anti-rabbit (#A-11034) Alexa Fluor 488 secondary antibodies were purchased from Invitrogen.

### *Human autophagy $RT^2$ Profiler™ PCR array*

To analyze gene expression, RNA was isolated from cells by using ISOGEN II (#317-07361, NIPPON GENE). The concentration of RNA was determined using a NanoDrop 2000 spectrophotometer (Thermo Fisher Scientific), and 1 μg of RNA was used to generate cDNA using the $RT^2$ First Strand Kit (#330401, SABiosciences, a Qiagen Company). The human autophagy $RT^2$ Profiler™ PCR array was used according to the manufacturer's instructions (#PAHS-084Z, SABiosciences) [14]. This PCR array profiled the expression of 84 key genes involved in autophagy (Supplementary Table 1) and exhibited good reproducibility of data. The fold change of expression was calculated using the SABiosciences web-based data analysis program. The results represent the mean of three independent samples.

### *RNA interference*

siRNA specific to ATG7 (#6604S) and a negative control siRNA (#6568S) were obtained from Cell Signaling Technology. siRNA specific to BNIP3L (#HSS101074) was obtained from Thermo Fisher Scientific. Transfections were performed using Lipofectamine 3000 transfection reagent (#L3000015, Invitrogen) according to the manufacturer's instructions. Briefly, we seeded cells in 6-well plates ($2 \times 10^5$ cells/well) for 16 h, and then added ATG7 siRNA (100 nM) or BNIP3L siRNA (20 nM). Two days after siRNA transfection, cells were treated with 10 μM DXR for another 24 h.

### *Western blotting*

Preparation of cell lysates and Western blotting analysis were performed following protocols previously described [13]. Briefly, cells were lysed at 4 °C in lysis buffer. Total proteins were separated by SDS-PAGE gels and then transferred to 0.22-μm PVDF membranes (Bio-Rad). After blocking, the membranes were incubated with indicated antibodies. The expression was visualized using an ECL detection kit (#RPN2106, GE Healthcare Life Sciences), and semi-quantitative analysis was performed by measuring the density of the bands using ImageQuant LAS 4000 Mini biomolecular imager (GE Healthcare Life Sciences).

### *Determination of $O_2^-$ production*

$O_2^-$ production was measured using MitoSOX Red reagent (#M36008, Invitrogen). Briefly, cells were incubated with 5 μM MitoSOX Red reagent for 10 min in the dark. After washing, the immunofluorescence in cells was analyzed on a FACSCalibur instrument (Becton Dickinson).

### *Immunofluorescence*

Immunofluorescence for LC3B and TOMM20 were performed following protocols previously described [13]. Briefly, cells were fixed with 4% formalin (#163-20145, Wako) for 10 min at room temperature. After blocking, cells were incubated with rabbit anti-human LC3B antibody (1:200 dilution) and mouse anti-human TOMM20 antibody (1:50 dilution) overnight at 4 °C. After washing three times with PBS, cells were incubated with anti-rabbit Alexa Fluor 488 (1:200 dilution) and anti-mouse Alexa Fluor 546 (1:200 dilution) secondary antibodies at room temperature for 1 h in the dark. The immunofluorescence in cells was examined on a laser confocal microscope (FV10i, Olympus). The mean number of LC3B puncta from more than 50 cells was calculated.

### *Statistical analysis*

The data are represented as the mean ± SD. Statistical analyses were performed using one-way analysis of variance (ANOVA) followed by a post hoc test (Dr. SPSS II, Chicago, IL). A $p$ value less than 0.05 was accepted as statistically significant.

## Results

### *$CD133^+/CD44^+$ CSCs were more resistant to DXR than parental cells*

We isolated the $CD133^+/CD44^+$ CSCs from parental HCT8 cells, and the purity was more than 95% by flow cytometry analysis (Supplementary Fig. 1). The expression of CD133 and CD44 in the purified CSCs was stable for at least 45 days after culture (Supplementary Fig. 1). After treatment with 10 μM DXR for 24 h, both CSCs and parental cells stopped growing, and many dead cells were observed to be floating in the medium (Fig. 1A). There were distinctly more surviving cells in the CSC cultures than in the parental cultures (Fig. 1A). An MTT assay clearly indicated the cell toxicity of DXR, and the cell viability was significantly higher in CSCs than parental cells (Fig. 1B). Apoptosis was also significantly

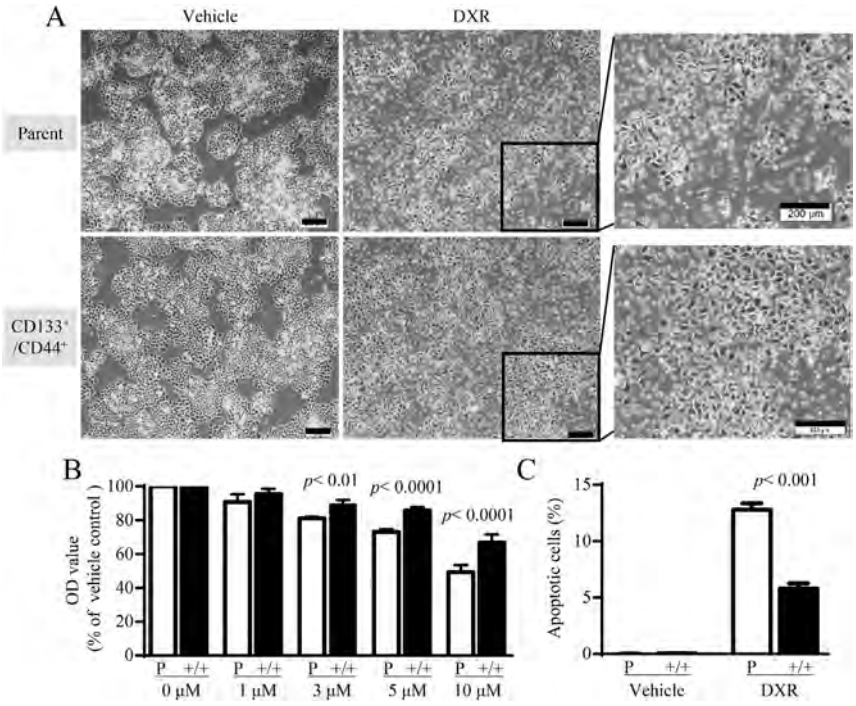


**Fig. 1.** *Cell survival and apoptosis.* (A) Cells were treated with 10 μM doxorubicin (DXR) for 24 h. The growth of cells was observed under a microscope with 40-fold magnification. Scale bars: 200 μm. (B) Cells were treated with various concentrations (0, 1, 3, 5 and 10 μM) of DXR for 24 h. The optical density (OD) value of cells with vehicle treatment was considered as 100% viability. (C) Cells were treated with 10 μM DXR for 24 h. Quantitative analysis of the apoptosis rate is shown. Parent or P: parental cells. $CD133^+/CD44^+$ or +/+: $CD133^+/CD44^+$ cells. The data are represented as the mean ± SD from three independent experiments.

induced after treatment with 10 μM DXR for 24 h, and a significantly lower apoptosis rate was observed in CSCs compared to parental cells (Fig. 1C).

Western blot analysis showed that DXR induced the apoptosis-related proteins cleaved PARP and cleaved caspase-3 in a dose- and time-dependent manner in both cell types (Fig. 2A,B). Quantitative data showed that the expression of cleaved PARP and cleaved caspase-3 was significantly lower in CSCs than in parental cells after treatment with 10 μM DXR for 24 h (Fig. 2C). The expression of cleaved caspase-7 was also significantly lower in CSCs than in parental cells after treatment with 10 μM DXR for 24 h (Fig. 2D).

### *DXR-induced autophagy in CSCs did not significantly contribute to drug resistance*

DXR-induced autophagy was increased with time in both cell types (Fig. 3A), and the autophagy level was obviously higher in

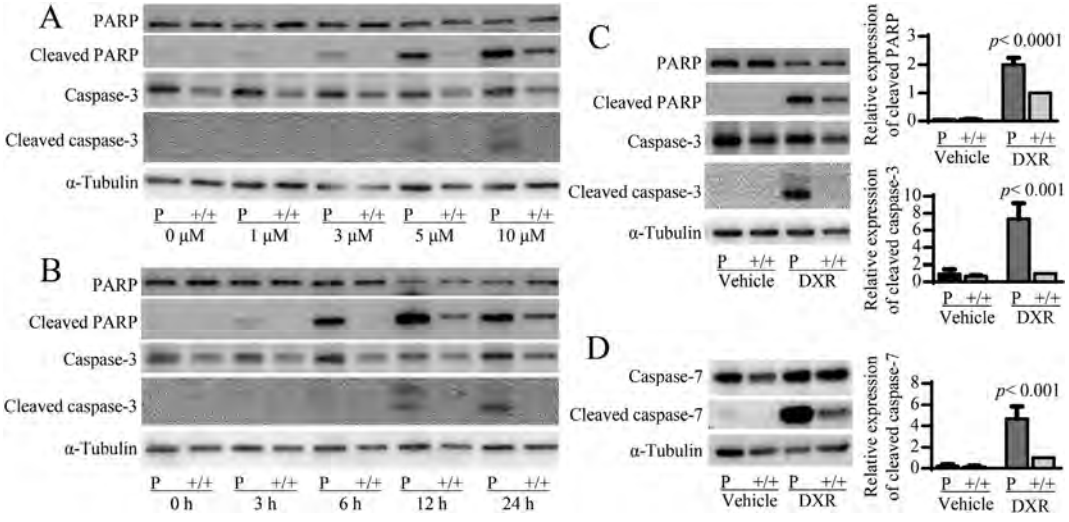


**Fig. 2.** *Western blot analysis of the expression of apoptosis related proteins.* (A) The expression of cleaved PARP and cleaved caspase-3 in cells after treatment with different concentrations (0, 1, 3, 5 and 10 μM) of doxorubicin (DXR) for 24 h. (B) The time-course changes of the expression of cleaved PARP and cleaved caspase-3 in cells after treatment with 10 μM DXR. (C) Quantitative analysis of the expression of cleaved PARP and cleaved caspase-3 after treatment with 10 μM DXR for 24 h. (D) Quantitative analysis of the expression of cleaved caspase-7 after treatment with 10 μM DXR for 24 h. P: parental cells. +/+: $CD133^+/CD44^+$ cells. The data are normalized to α-tubulin and represented as the mean ± SD from three independent experiments.

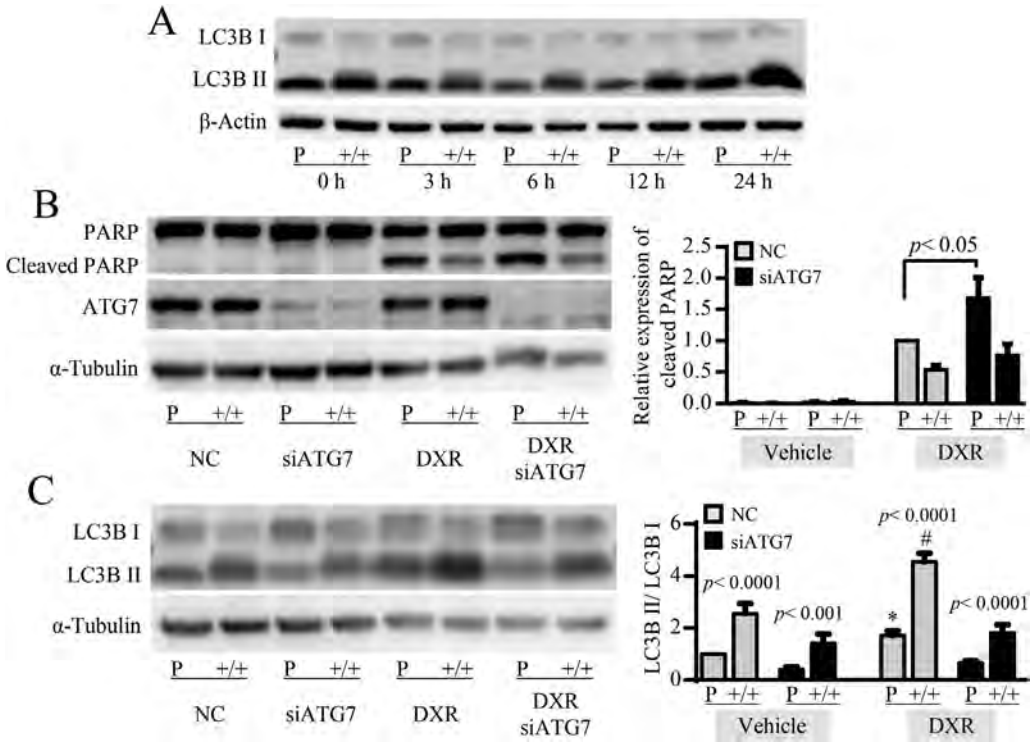


**Fig. 3.** *Autophagy and doxorubicin resistance in cells.* (A) The time-course changes of the expression of LC3B in cells after 10 μM doxorubicin (DXR) treatment. (B) After treatment and 2-day incubation with ATG7 siRNA, cells were treated with 10 μM DXR for another 24 h. Western blot analysis of the expression of cleaved PARP and ATG7. (C) After treatment and 2-day incubation with ATG7 siRNA, cells were treated with 10 μM DXR for another 24 h. Western blot analysis of the expression of LC3B. *: $p < 0.01$ *vs.* parental cells without treatment, #: $p < 0.0001$ *vs.* $CD133^+/CD44^+$ cells without treatment. NC: negative control siRNA. P: parental cells. +/+: $CD133^+/CD44^+$ cells. The data are normalized to α-tubulin and represented as the mean ± SD from three independent experiments.

CSCs than in parental cells (Fig. 3A,C). To investigate the role of autophagy in the DXR resistance in CSCs, we analyzed the effect of silencing ATG7, a factor required for autophagy. Transfection with ATG7 siRNA clearly reduced the protein level of ATG7 (Fig. 3B). Surprisingly, ATG7 silencing significantly enhanced the expression of cleaved PARP in parental cells, but not in CSCs, after treatment with 10 μM DXR for 24 h (Fig. 3B), although ATG7 silencing clearly decreased the ratio of LC3B-II/LC3B-I in both cell types (Fig. 3C).

We also investigated the expression of autophagy-related genes by human $RT^2$ Profiler™ PCR array (Fig. 4, Supplementary Table 2 and Supplementary Table 3). At the basal level, some autophagy-related genes were highly expressed in CSCs when compared to parental cells (Fig. 4A). Interestingly, treatment with 10 μM DXR for 24 h up-regulated the autophagy-related genes more extensively in parental cells (Fig. 4B) than in CSCs (Fig. 4C), which resulted in comparable expression levels in autophagy-related genes between CSCs and parental cells (Fig. 4D).

### *DXR treatment induced mitophagy more extensively in CSCs than in parental cells*

Following DXR treatment, mitochondrial membrane protein TOMM20 decreased with time in both cell types (Fig. 5A). Western blot analysis showed that the basal level of TOMM20 was not significantly different between the two cell types (Fig. 5B), but CSCs had significantly less TOMM20 than parental cells 24 h after DXR treatment (Fig. 5B). The mitochondrial superoxide was quantitatively measured by fluorescence intensity after loading with mitoSOX. Although the mitochondrial superoxide level significantly increased in both cell types 24 h after DXR treatment (Fig. 5C), there was a significantly lower mitochondrial superoxide level in CSCs than in parental cells (Fig. 5C). Confocal microscopy analysis showed that LC3B puncta were significantly increased by DXR treatment in both cell types, but the number of LC3B puncta was significantly higher in CSCs than in parental cells (Fig. 5D,E). In addition, the co-localization of mitochondria (TOMM20) and autophagosomes (LC3B) was significantly increased in CSCs compared to parental cells after DXR treatment, indicating a higher level of mitophagy in CSCs than in parental cells (Fig. 5D,F).

We further investigated the expression of several factors known to be closely associated with mitophagy. The expression of parkin and PINK1 was not significantly different between the two cell types, even after DXR treatment (Supplementary Fig. 2A and B). The phosphorylation level of ERK1/2 was significantly decreased in both cell types 24 h after DXR treatment (Supplementary Fig. 2C), but there was no significant difference between the two cell types (Supplementary Fig. 2C). However, the expression of BNIP3L was significantly higher in CSCs than in parental cells (Fig. 6A), and further increased with time in both cell types after DXR treatment (Fig. 6B).

### *Inhibition of mitophagy significantly improved the sensitivity of DXR in CSCs*

To further investigate the relationship between mitophagy and DXR resistance in CSCs, we silenced the expression of BNIP3L, a key regulator of mitophagy [6]. Transfection with BNIP3L siRNA significantly decreased the protein level of BNIP3L in both CSCs and parental cells (Fig. 6C), but it did not significantly change the autophagy level in either cell type (Fig. 6D). Western blot analysis showed that the knockdown of BNIP3L significantly enhanced the expression of cleaved PARP in CSCs after DXR treatment (Fig. 6E).

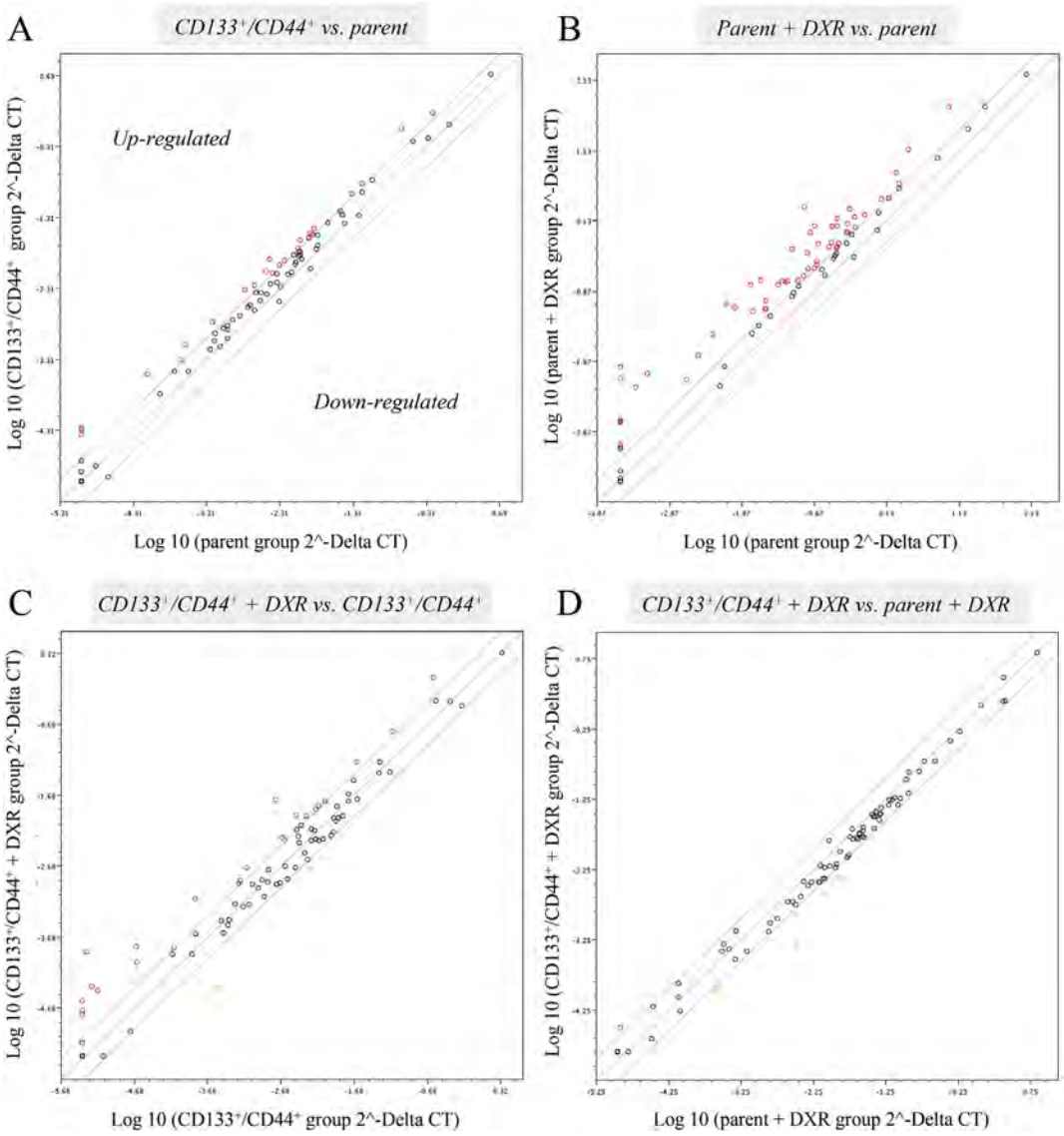


**Fig. 4.** *Pathway-focused PCR array.* The expression of autophagy-related genes was measured in cells with or without doxorubicin (DXR) treatment for 24 h. Red circles represent up-regulated genes with more than a two-fold change, whereas the green circles represent down-regulated genes with more than a two-fold change. (A) The comparison of gene expression profiles between $CD133^+/CD44^+$ cells and parental cells at basal level (without DXR treatment). (B) The comparison of gene expression profiles in parental cells with or without DXR treatment. (C) The comparison of gene expression profiles in $CD133^+/CD44^+$ cells with or without DXR treatment. (D) The comparison of gene expression profiles between $CD133^+/CD44^+$ cells and parental cells after treatment with DXR. Parent: parental cells. $CD133^+/CD44^+$: $CD133^+/CD44^+$ cells. (For interpretation of the references to colour in this figure legend, the reader is referred to the web version of this article.)

Confocal microscopy analysis showed that BNIP3L silencing did not significantly change the total number of LC3B puncta in either cell type (Fig. 7A,C), but the DXR-induced mitochondrial localization of LC3B puncta was significantly decreased in cells with BNIP3L silencing (Fig. 7B,C).

## Discussion

Drug resistance is a major cause of tumor recurrence, metastasis and poor clinical outcome in cancer patients [15,16], and there is increasing evidence of drug resistance in CSCs [3,17,18]. The data from the present study confirmed that $CD133^+/CD44^+$ CSCs were more resistant to DXR than parental HCT8 colorectal cancer cells.

Recently, it has been reported that DXR strongly binds to mitochondria, which thereby increases mitochondrial superoxide and mitochondrial-mediated apoptosis [10,19]. In this study, fewer mitochondria and lower levels of mitochondrial superoxide were found in CSCs than in parental cells, implying excessive mitochondrial clearance in CSCs. Although the excessive mitochondrial clearance may induce cell metabolic disorders and cell death, the remarkable metabolic plasticity of CSCs is more likely to lead to cell survival [20,21]. In fact, the drug resistance of cancer cells can be due to a metabolic shift from oxidative phosphorylation to a high rate of glycolysis, which ultimately protects cancer cells from mitochondrial superoxide [22]. After DXR treatment, we observed a higher level of mitophagy in CSCs than in parental cells. Mitophagy, a selective autophagic mitochondria clearance pathway, is known to be critical in mitochondrial quality control [5,23,24]. DXR-induced mitophagy may facilitate cell survival by clearing the damaged mitochondria in CSCs.

To further confirm the causal relationship between mitophagy and DXR resistance in CSCs, we investigated the expression of

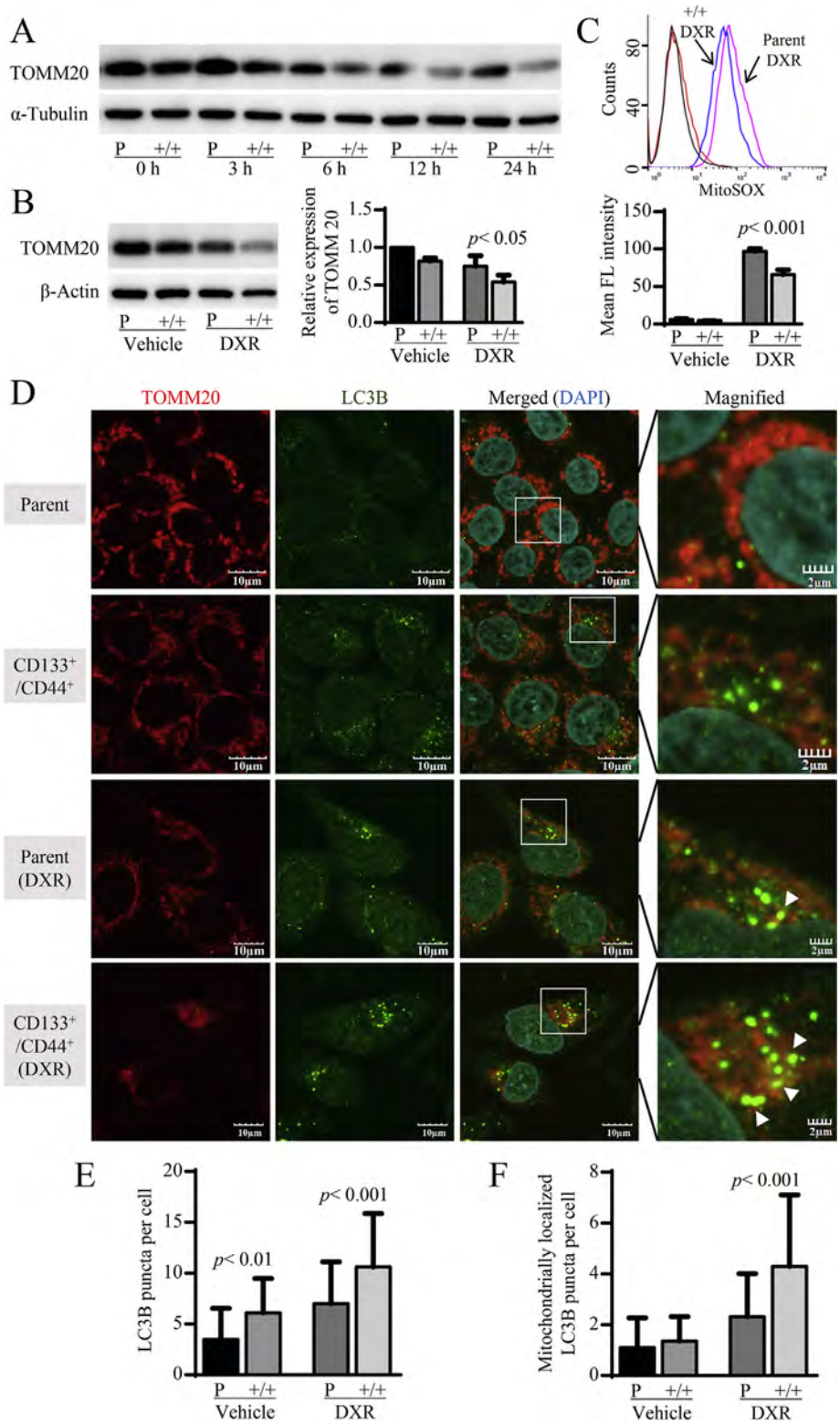


**Fig. 5.** *Mitochondria and mitophagy levels in cells.* (A) The time-course changes of the expression of TOMM20 after 10 μM doxorubicin (DXR) treatment. (B) Quantitative analysis of the expression of TOMM20 after treatment with 10 μM DXR for 24 h. The data are normalized to β-actin. (C) Cells were treated with 10 μM DXR for 24 h, and flow cytometry analysis was used to measure the mitochondrial superoxide level. The bar graph in the lower panel shows the quantitative data of mean fluorescence intensity. Parent cells: black line; $CD133^+/CD44^+$ cells: red line; Parent cells with DXR treatment: purple line; $CD133^+/CD44^+$ cells with DXR treatment: blue line. (D) Cells were treated with 10 μM DXR for 24 h, and confocal microscopy analysis of the co-localization of LC3B and TOMM20 was performed. Scale bars, 10 μm (Scale bars of magnified images are 2 μm). (E) Quantitative analysis of LC3B puncta per cell. (F) Quantitative analysis of mitochondrially localized LC3B puncta per cell. Parent or P: parental cells. $CD133^+/CD44^+$ or +/+: $CD133^+/CD44^+$ cells. The data are represented as the mean ± SD from three independent experiments. (For interpretation of the references to colour in this figure legend, the reader is referred to the web version of this article.)

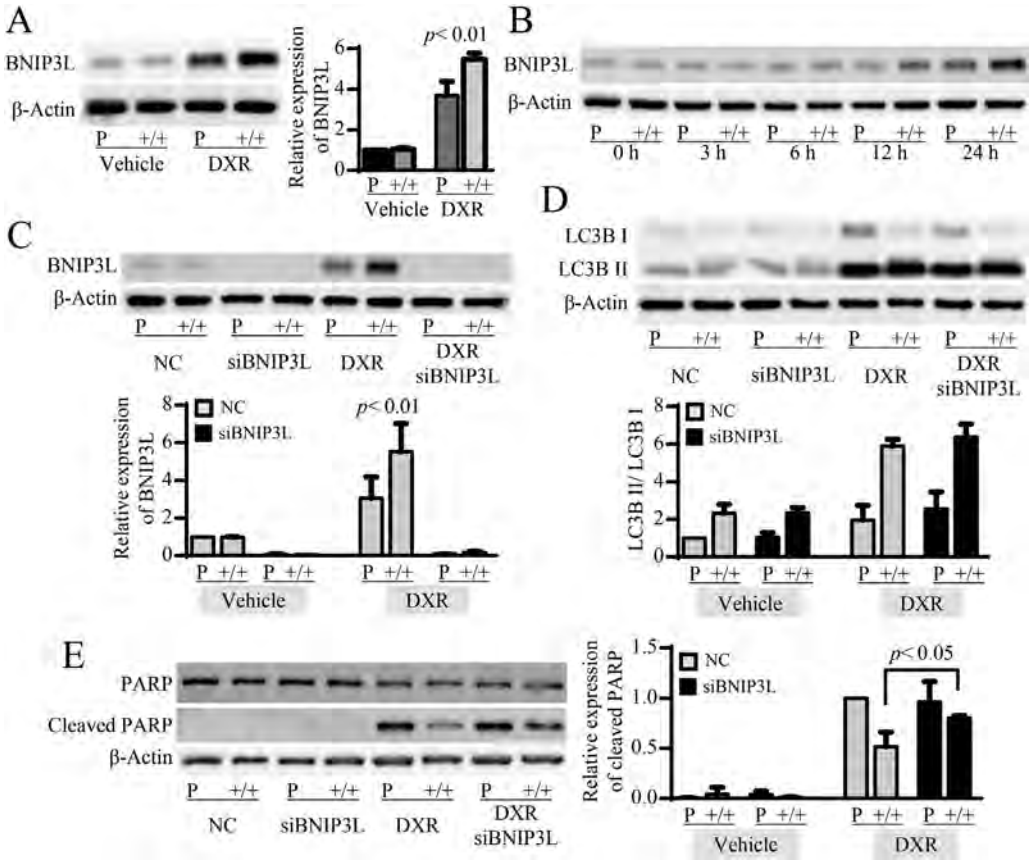


**Fig. 6.** *Relationship between the expression of BNIP3L and doxorubicin resistance.* (A) Cells were treated with 10 μM doxorubicin (DXR) for 24 h. Western blot analysis of the expression BNIP3L. (B) The time-course changes of the expression of BNIP3L after 10 μM DXR treatment. (C) After treatment and 2-day incubation with BNIP3L siRNA, cells were treated with 10 μM DXR for another 24 h. Western blot analysis of the expression of BNIP3L. (D) After treatment and 2-day incubation BNIP3L siRNA, cells were treated with 10 μM DXR for another 24 h. Western blot analysis of the expression of LC3B. (E) After treatment and 2-day incubation with BNIP3L siRNA, cells were treated with 10 μM DXR for another 24 h. Western blot analysis of the expression of cleaved PARP. NC: negative control siRNA. P: parental cells. +/+: $CD133^+/CD44^+$ cells. The data are normalized to β-actin and represented as the mean ± SD from three independent experiments.

mitophagy regulators PINK1, parkin, BNIP3L, and phosphorylated ERK1/2 [23–28]. Interestingly, DXR treatment only triggered a rapid increase of BNIP3L protein level in CSCs. Furthermore, the knockdown of BNIP3L significantly halted DXR-induced mitophagy and enhanced the toxicity of DXR in CSCs. In view of these results, we speculated that the activation of mitophagy by BNIP3L might improve cell survival and confer DXR resistance in CSCs. As the inhibition of BNIP3L expression only partially improved the DXR resistance of CSCs, other pro-survival pathways could also be involved in DXR resistance of CSCs. In fact, some cell death inducers, such as DAPK1, FADD and TNFSF10 [29–31], were poorly expressed in CSCs after DXR treatment (Supplementary Table 2), which might promote the survival of CSCs.

The function of autophagy in the therapeutic resistance of cancer is still ambiguous [32]. It has been previously reported that autophagy contributes to drug resistance in cancer cells [33–35]. In this study, we also confirmed that the inhibition of autophagy can enhance DXR sensitivity in parental cells. Compared with the parental cells, the CSCs always had more of the lipidated form of LC3B (LC3B-II) and less of the cytosolic form of LC3B (LC3B-I) (Fig. 3A). As LCB3-II is a commonly used marker of autophagosomes [36], this result indicates an increased number of autophagosomes and an enhanced activity of autophagy in CSCs. However, the inhibition of autophagy by ATG7 silencing did not significantly attenuate the DXR resistance of CSCs. Although ATG proteins are thought to be crucial for autophagy, ATG7-independent autophagy was observed in ATG7 knockout cells [25,37]. As mitophagy is primarily due to ATG7-independent autophagy [25,27], the knockdown of ATG7 may induce only minor changes in mitophagy.

It is not clear why mitophagy, but not non-selective autophagy, contributes to DXR resistance in CSCs. Our data from a PCR array analysis showed that DXR treatment weakly stimulated autophagy-related genes in CSCs (Fig. 4C). We have very recently found that canonical autophagy plays few roles in the radioresistance of CSCs [13]. In addition to DXR, we also tested another chemotherapeutic agent, cisplatin, and observed resistance in the CSCs. However, the cisplatin did not induce mitophagy (data not shown). As different chemotherapeutic agents have different anti-cancer mechanisms, the cisplatin resistance of CSCs might depend on other mechanisms rather than mitophagy. This study is largely limited by using a single cell line. We attempted to isolate $CD133^+/CD44^+$ cells from several other cancer cell lines, such as COLO320, A549 and HeLa cells. However, we failed to collect $CD133^+/CD44^+$ cells from these cell lines due to various difficulties, such as insufficient cell purity and instability of cell surface marker expression during the culture process after cell purification.

In conclusion, we demonstrated that mitophagy, but not non-selective autophagy, likely plays a key role in conferring DXR resistance in CSCs isolated from HCT8 human colorectal cancer cells. Taking past studies into consideration [4,8,25], we propose that in response to chemotherapy, mitophagy is activated in CSCs to clear the damaged mitochondria, which consequently results in

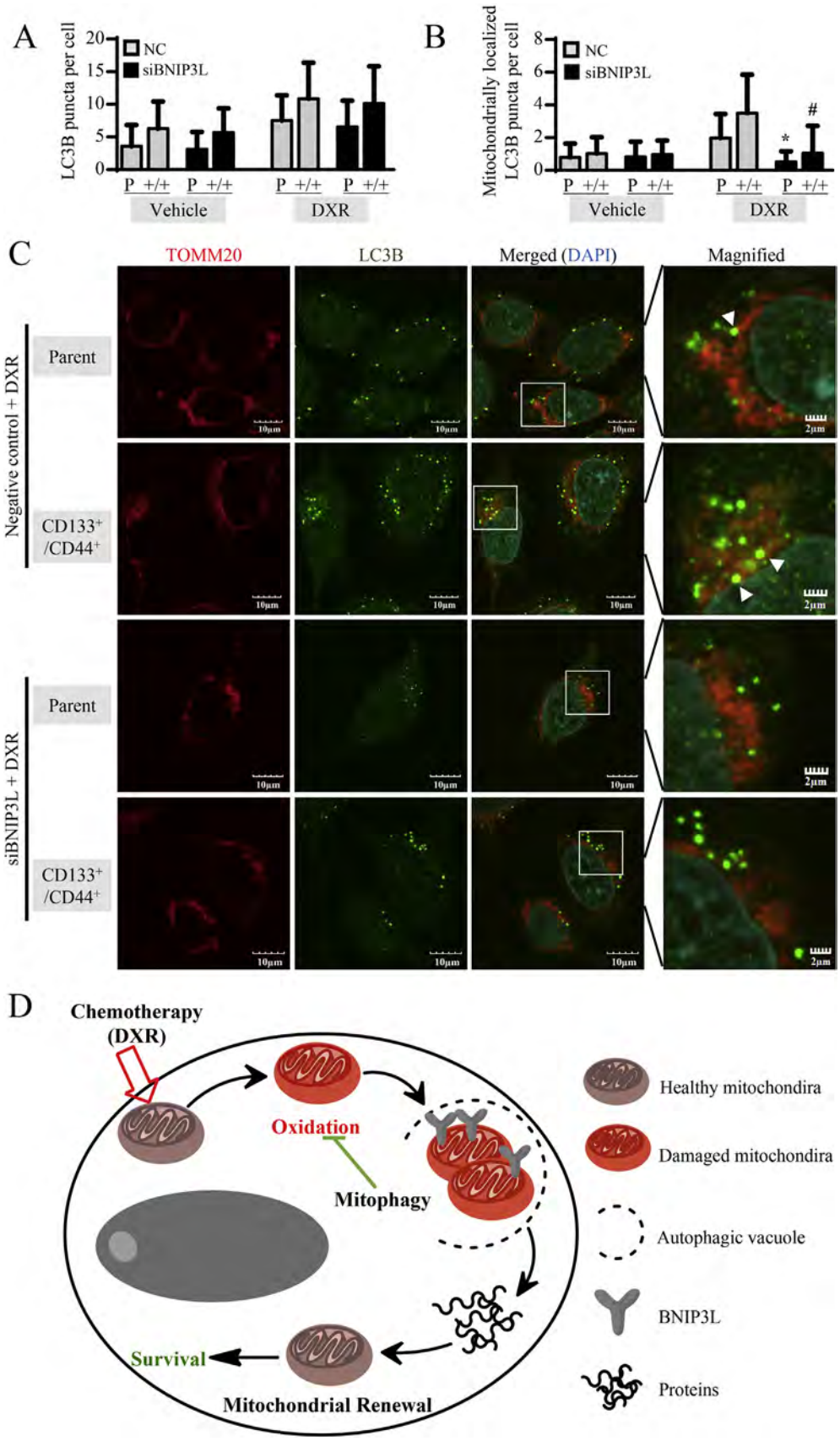


**Fig. 7.** *Knockdown of BNIP3L changes mitophagy and doxorubicin resistance in cells.* After treatment and 2-day incubation with BNIP3L siRNA, cells were treated with 10 μM doxorubicin (DXR) for another 24 h. (A) Quantitative analysis of LC3B puncta per cell. (B) Quantitative analysis of mitochondrially localized LC3B puncta per cell, *: $p < 0.0001$ *vs.* parent cells with DXR treatment, #: $p < 0.0001$ *vs.* $CD133^+/CD44^+$ cells with DXR treatment. (C) Confocal microscopy analysis of the co-localization of LC3B and TOMM20. Scale bars, 10 μm (Scale bars of magnified images are 2 μm). (D) The potential effect of mitophagy on the drug resistance of cancer stem cells. NC: negative control siRNA. Parent or P: parental cells. $CD133^+/CD44^+$ or +/+: $CD133^+/CD44^+$ cells. The data are represented as the mean ± SD from three independent experiments.

reduced oxidative stress and finally contributes to cell survival (Fig. 7D). Further studies are warranted to elucidate how mitophagy is regulated in CSCs, which may inform the development of novel strategies for the treatment of cancers.

## Acknowledgments and grant support

This study was supported in part by a Grant-in-Aid from the Ministry of Education, Science, Sports, Culture and Technology, Japan (NO. 26293279), and the Collaborative Research Program of the Atomic-bomb Disease Institute of Nagasaki University. The funder played no role in the study design, the data collection and analysis, decision to publish, or preparation of the manuscript.

## Disclosure of potential conflicts of interest

The authors declare no conflict of interest.

## Appendix A. Supplementary data

Supplementary data related to this article can be found at http://dx.doi.org/10.1016/j.canlet.2016.11.018.

## References

[1] J.E. Visvader, G.J. Lindeman, Cancer stem cells: current status and evolving complexities, Cell Stem Cell. 10 (2012) 717–728, http://dx.doi.org/10.1016/j.stem.2012.05.007.
[2] S.J. Dylla, L. Beviglia, I.K. Park, C. Chartier, J. Raval, L. Ngan, et al., Colorectal cancer stem cells are enriched in xenogeneic tumors following chemotherapy, PLoS One 3 (2008) e2428, http://dx.doi.org/10.1371/journal.pone.0002428.
[3] M.L. De Angelis, A. Zeuner, E. Policicchio, G. Russo, A. Bruselles, M. Signore, et al., Cancer stem cell-based models of colorectal cancer reveal molecular determinants of therapy resistance, Stem Cells Transl. Med. 5 (2016) 511–523, http://dx.doi.org/10.5966/sctm.2015-0214.
[4] S. Vyas, E. Zaganjor, M.C. Haigis, Mitochondria and cancer, Cell 166 (2016) 555–566, http://dx.doi.org/10.1016/j.cell.2016.07.002.
[5] R.J. Youle, D.P. Narendra, Mechanisms of mitophagy, Nat. Rev. Mol. Cell Biol. 12 (2011) 9–14, http://dx.doi.org/10.1038/nrm3028.
[6] H. Lu, G. Li, L. Liu, L. Feng, X. Wang, H. Jin, Regulation and function of mitophagy in development and cancer, Autophagy 9 (2013) 1720–1736, http://dx.doi.org/10.4161/auto.26550.
[7] H. Maes, P. Agostinis, Autophagy and mitophagy interplay in melanoma progression, Mitochondrion 19 (Pt A) (2014) 58–68, http://dx.doi.org/10.1016/j.mito.2014.07.003.
[8] J. Zhou, G. Li, Y. Zheng, H.M. Shen, X. Hu, Q.L. Ming, et al., A novel autophagy/mitophagy inhibitor liensinine sensitizes breast cancer cells to chemotherapy through DNM1L-mediated mitochondrial fission, Autophagy 11 (2015) 1259–1279, http://dx.doi.org/10.1080/15548627.2015.1056970.
[9] N. Ashley, J. Poulton, Mitochondrial DNA is a direct target of anti-cancer anthracycline drugs, Biochem. Biophys. Res. Commun. 378 (2009) 450–455, http://dx.doi.org/10.1016/j.bbrc.2008.11.059.
[10] S. Zhang, X. Liu, T. Bawa-Khalfe, L.S. Lu, Y.L. Lyu, L.F. Liu, et al., Identification of the molecular basis of doxorubicin-induced cardiotoxicity, Nat. Med. 18 (2012) 1639–1642, http://dx.doi.org/10.1038/nm.2919.
[11] S. Luanpitpong, P. Chanvorachote, U. Nimmannit, S.S. Leonard, C. Stehlik, L. Wang, et al., Mitochondrial superoxide mediates doxorubicin-induced keratinocyte apoptosis through oxidative modification of ERK and Bcl-2 ubiquitination, Biochem. Pharmacol. 83 (2012) 1643–1654, http://dx.doi.org/10.1016/j.bcp.2012.03.010.
[12] N. Haraguchi, M. Ohkuma, H. Sakashita, S. Matsuzaki, F. Tanaka, K. Mimori, et al., CD133+CD44+ population efficiently enriches colon cancer initiating cells, Ann. Surg. Oncol. 15 (2008) 2927–2933, http://dx.doi.org/10.1245/s10434-008-0074-0.
[13] C. Yan, L. Luo, S. Goto, Y. Urata, C.Y. Guo, H. Doi, et al., Enhanced autophagy in colorectal cancer stem cells does not contribute to radio-resistance, Oncotarget 7 (2016) 45112–45121, http://dx.doi.org/10.18632/oncotarget.8972.
[14] H. Ali, O. Galal, Y. Urata, S. Goto, C.Y. Guo, L. Luo, et al., The potential benefits of nicaraven to protect against radiation-induced injury in hematopoietic stem/progenitor cells with relative low dose exposures,, Biochem. Biophys. Res. Commun. 452 (2014) 548–553, http://dx.doi.org/10.1016/j.bbrc.2014.08.112.
[15] O. Tredan, C.M. Galmarini, K. Patel, I.F. Tannock, Drug resistance and the solid tumor microenvironment, J. Natl. Cancer Inst. 99 (2007) 1441–1454, http://dx.doi.org/10.1093/jnci/djm135.
[16] C. Holohan, S. Van Schaeybroeck, D.B. Longley, P.G. Johnston, Cancer drug resistance: an evolving paradigm, Nat. Rev. Cancer 13 (2013) 714–726, http://dx.doi.org/10.1038/nrc3599.
[17] B.B. Zhou, H. Zhang, M. Damelin, K.G. Geles, J.C. Grindley, P.B. Dirks, Tumour-initiating cells: challenges and opportunities for anticancer drug discovery, Nat. Rev. Drug Discov. 8 (2009) 806–823, http://dx.doi.org/10.1038/nrd2137.
[18] R. Lamb, H. Harrison, J. Hulit, D.L. Smith, M.P. Lisanti, F. Sotgia, Mitochondria as new therapeutic targets for eradicating cancer stem cells: quantitative proteomics and functional validation via MCT1/2 inhibition, Oncotarget 5 (2014) 11029–11037, http://dx.doi.org/10.18632/oncotarget.2789.
[19] N. Yadav, S. Kumar, T. Marlowe, A.K. Chaudhary, R. Kumar, J. Wang, et al., Oxidative phosphorylation-dependent regulation of cancer cell apoptosis in response to anticancer agents, Cell Death Dis. 6 (2015) e1969, http://dx.doi.org/10.1038/cddis.2015.305.
[20] Y.A. Shen, C.Y. Wang, Y.T. Hsieh, Y.J. Chen, Y.H. Wei, Metabolic reprogramming orchestrates cancer stem cell properties in nasopharyngeal carcinoma, Cell Cycle 14 (2015) 86–98, http://dx.doi.org/10.4161/15384101.2014.974419.
[21] E. Vlashi, F. Pajonk, The metabolic state of cancer stem cells-a valid target for cancer therapy?,, Free Radic. Biol. Med. 79 (2015) 264–268, http://dx.doi.org/10.1016/j.freeradbiomed.2014.10.732.
[22] M.E. Harper, A. Antoniou, E. Villalobos-Menuey, A. Russo, R. Trauger, M. Vendemelio, et al., Characterization of a novel metabolic strategy used by drug-resistant tumor cells, FASEB J. 16 (2002) 1550–1557, http://dx.doi.org/10.1096/fj.02-0541com.
[23] G.L. McLelland, V. Soubannier, C.X. Chen, H.M. McBride, E.A. Fon, Parkin and PINK1 function in a vesicular trafficking pathway regulating mitochondrial quality control, EMBO J. 33 (2014) 282–295, http://dx.doi.org/10.1002/embj.201385902.
[24] H. Sandoval, P. Thiagarajan, S.K. Dasgupta, A. Schumacher, J.T. Prchal, M. Chen, et al., Essential role for Nix in autophagic maturation of erythroid cells, Nature 454 (2008) 232–235, http://dx.doi.org/10.1038/nature07006.
[25] P.A. Ney, Mitochondrial autophagy: origins, significance, and role of BNIP3 and NIX, Biochim. Biophys. Acta 1853 (2015) 2775–2783, http://dx.doi.org/10.1016/j.bbamcr.2015.02.022.
[26] F. Gao, D. Chen, J. Si, Q. Hu, Z. Qin, M. Fang, et al., The mitochondrial protein BNIP3L is the substrate of PARK2 and mediates mitophagy in PINK1/PARK2 pathway, Hum. Mol. Genet. 24 (2015) 2528–2538, http://dx.doi.org/10.1093/hmg/ddv017.
[27] Y. Hirota, S. Yamashita, Y. Kurihara, X. Jin, M. Aihara, T. Saigusa, et al., Mitophagy is primarily due to alternative autophagy and requires the MAPK1 and MAPK14 signaling pathways, Autophagy 11 (2015) 332–343, http://dx.doi.org/10.1080/15548627.2015.1023047.
[28] L. Liu, K. Sakakibara, Q. Chen, K. Okamoto, Receptor-mediated mitophagy in yeast and mammalian systems, Cell Res. 24 (2014) 787–795, http://dx.doi.org/10.1038/cr.2014.75.
[29] W. He, Q. Wang, J. Xu, X. Xu, M.T. Padilla, G. Ren, et al., Attenuation of TNFSF10/TRAIL-induced apoptosis by an autophagic survival pathway involving TRAF2- and RIPK1/RIP1-mediated MAPK8/JNK activation, Autophagy 8 (2012) 1811–1821, http://dx.doi.org/10.4161/auto.22145.
[30] A. Raval, S.M. Tanner, J.C. Byrd, E.B. Angerman, J.D. Perko, S.S. Chen, et al., Downregulation of death-associated protein kinase 1 (DAPK1) in chronic lymphocytic leukemia, Cell. 129 (2007) 879–890, http://dx.doi.org/10.1016/j.cell.2007.03.043.
[31] L. Tourneur, G. Chiocchia, FADD: a regulator of life and death, Trends Immunol. 31 (2010) 260–269, http://dx.doi.org/10.1016/j.it.2010.05.005.
[32] D.A. Gewirtz, The four faces of autophagy: implications for cancer therapy, Cancer Res. 74 (2014) 647–651, http://dx.doi.org/10.1158/0008-5472.CAN-13-2966.
[33] V.B. Yenigun, B. Ozpolat, G.T. Kose, Response of CD44+/CD24-/low breast cancer stem/progenitor cells to tamoxifen and doxorubicininduced autophagy, Int. J. Mol. Med. 31 (2013) 1477–1483, http://dx.doi.org/10.3892/ijmm.2013.1342.
[34] X. Li, D. Roife, Y. Kang, B. Dai, M. Pratt, J.B. Fleming, Extracellular lumican augments cytotoxicity of chemotherapy in pancreatic ductal adenocarcinoma cells via autophagy inhibition, Oncogene 35 (2016) 4881–4890, http://dx.doi.org/10.1038/onc.2016.20.
[35] Z.J. Yang, C.E. Chee, S. Huang, F.A. Sinicrope, The role of autophagy in cancer: therapeutic implications, Mol. Cancer Ther. 10 (2011) 1533–1541, http://dx.doi.org/10.1158/1535-7163.MCT-11-0047.
[36] D.J. Klionsky, K. Abdelmohsen, A. Abe, M.J. Abedin, H. Abeliovich, A. Acevedo Arozena, et al., Guidelines for the use and interpretation of assays for monitoring autophagy (3rd edition), Autophagy 12 (2016) 1–222, http://dx.doi.org/10.1080/15548627.2015.1100356.
[37] Y. Nishida, S. Arakawa, K. Fujitani, H. Yamaguchi, T. Mizuta, T. Kanaseki, et al., Discovery of Atg5/Atg7-independent alternative macroautophagy, Nature 461 (2009) 654–658, http://dx.doi.org/10.1038/nature08455.